20dB-enhanced coupling to slot photonic crystal waveguide based on multimode interference

Xiaonan Chen[1], Lanlan Gu[2], Wei Jiang[2], and Ray T. Chen[1*]
Microelectronic Research Center, Department of Electrical and Computer Engineering,
[1]The University of Texas at Austin, Austin, TX 78758, USA
[2]Omega Optics Inc, Austin, TX 78758, USA
*** Email: chen@ece.utexas.edu**

ABSTRACT

We experimentally demonstrate a novel slot photonic crystal waveguide for guiding light with low group velocity in a 100-nm-wide low-index region. The unique optical property and structural features of the slotted photonic crystals best match the requirements for active material-based silicon devices. We integrate the novel photonic crystal waveguide with a multimode interference-based coupling structure and measure a 20dB efficiency enhancement compared with direct coupling configuration. The measured transmission spectra are in good agreement with simulated band diagram.

Keywords: slot photonic crystal waveguide, multimode interference, mode converter, active device.

I. INTRODUCTION

Photonic crystal waveguides (PCW) with low group velocity have been demonstrated recently to replace conventional optical switches and modulators [1-4], where the size of the active region is considerably reduced via slow light effect [5, 6]. They typically consist of a periodic array of air holes on a dielectric substrate whose optical properties are modified by an external physical signal. One of the most efficient tuning methods may be based on the application of electro-optical material. It is well known that the unique properties of photonic crystals can be exploited to enhance the nonlinear effect drastically and thus a small attainable change in the refractive index can induce applicable optical response [7]. In order to apply the improved electro-optical effects in waveguide devices and to satisfy the low power requirement, we need to excite a guided mode within a narrow active material region. A new type of integrated optical waveguide called slot waveguide opens the opportunity for guiding and confining light in a 100-nm-wide slot filled with low-refractive-index electro-optical materials [8, 9]. We embed such nanostructures in photonic crystals and design a novel slot PCW configuration in order to combine the unusual optical features of photonic crystals and slot waveguides. A compact multimode interference structure is integrated and optimized to maximize the coupling efficiency from strip waveguides to the slotted region. Other groups propose similar combination techniques by embedding dielectric waveguides into photonic crystal slabs and create large bandwidth and low dispersion within the photonic band-gap region [10].

Photonics Packaging, Integration, and Interconnects VIII, edited by Alexei L. Glebov, Ray T. Chen
Proc. of SPIE Vol. 6899, 68990Q, (2008) · 0277-786X/08/$18 · doi: 10.1117/12.768188

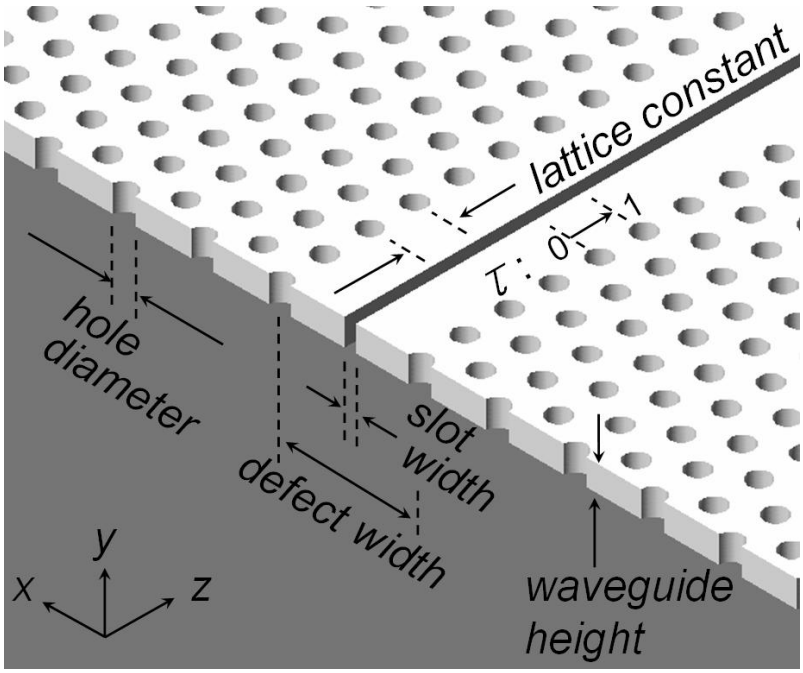

(a)

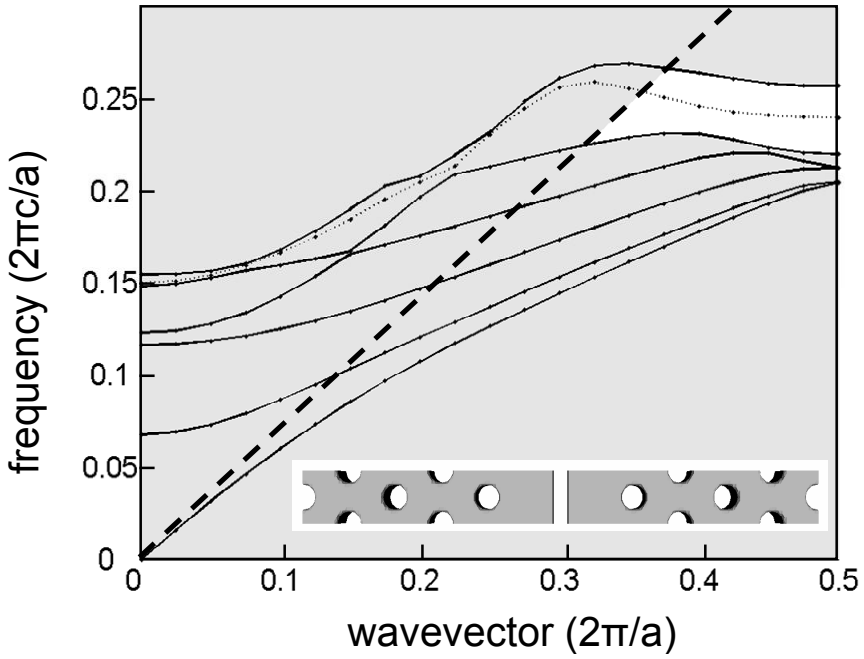

(b)

Fig. 1. (a) Line defect structure with a low-index nanometer-size center slot embedded in a photonic crystal slab. (b) Band diagram for slot photonic crystal wabeguides. The thick dashed line is the light line. The gray regions represent the continuum of extended modes. The dotted curve indicates the created defect mode. The inset shows the supercell model defined in PWE simulation.

II. DESIGN OF SLOT PHOTONIC CRYSTAL WAVEGUIDE

As shown in Fig. 1(a), a slotted photonic crystal slab, with high refractive index n_{Si}=3.48, is sandwiched between two low-index regions with n_{SiO2}=1.46. Theoretical analysis predicts that such photonic crystal structures with high index contrast in the vertical direction support an in-plane photonic band gap that lies below the light line [11, 12]. Defect modes within the gap region can be created by various line defects [13]. Here we generate the line defect in the photonic crystal slab by replacing a single row of holes with a narrow slot and enlarge the width of the defect region to create a relatively large effective core area of the waveguide. The scattering loss due to side-wall roughness can therefore be reduced with larger waveguide width [14]. As a wider defect region may induce multiple bands into the gap region, care must be taken to design the enlarged defect width [15].

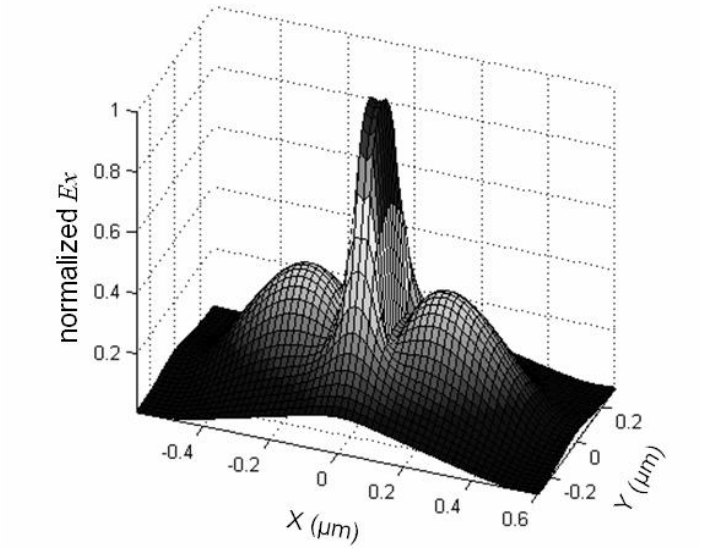

Fig. 2. 3D profile of the transverse electric field amplitude of the quasi-TE mode in a slot photonic crystal waveguide, where a=380nm, d=190nm, h=228nm, slot width=95nm, defect width=1053nm, n_{Si}=3.48 and n_{SLOT}=n_{SiO2}=1.46.

We apply the plane-wave expansion (PWE) method to calculate the dispersion diagram of the slot PCW. We assume that the hole diameter d=0.5a and the waveguide height h=0.6a, where a is the lattice constant of the photonic crystals. The results shown in Fig. 1(b) indicate that the slotted photonic crystals still have a single-mode region when the defect width is enlarged to 1.6W, where $W = \sqrt{3}a$ is the width of the normal line defect [16]. The guided mode is a quasi-TE mode with slow light effect near the band edge. Based on Maxwell's equations, when the transverse electric field of the quasi-TE mode (*Ex*) undergoes strong dielectric constant discontinuity of the slot walls, the immediate electric field is much higher at the low-index side [8]. It has been experimentally demonstrated that the field amplitude remains high all across the slot if the slot width is much smaller than the field decay length [9]. Based on the same operation principle, we set the slot width of the PCW to 0.25a and obtain high E-field confinement in the slot as shown in Fig. 2. Simulation is based on 3D finite-difference time-domain (FDTD) method. The structure features of the slot PCW nicely match the requirements for active material-based silicon devices: the guided mode produces high electric field in a low-index

region, creating an opportunity for various low-index electro-optical materials; the slow group velocity of the defect mode can drastically enhance the electro-optical effect and thereby open up the possibility of ultra-compact nonlinear devices. Moreover, as the width of the center slot region is less than 100nm, the novel photonic crystal structure provides a convenient way to generate sufficient external electric field for active materials with low driving voltage.

III. DESIGN AND OPTIMIZATION OF MULTIMODE INTERFERENCE COUPLER

The mode contour comparison of a slot PCW and a single-mode silicon strip waveguide is drawn in Fig. 3. Large coupling loss is inevitable for direct coupling due to the mode-size and mode-shape mismatch. A common solution is to introduce a single-mode to multi-mode waveguide taper structure. However, the tapering structure requires a minimal taper length of several hundred of microns to reduce the propagation loss due to mode transform. In order to implement a more compact mode converter, we integrate multimode interference-based coupling structures in our device.

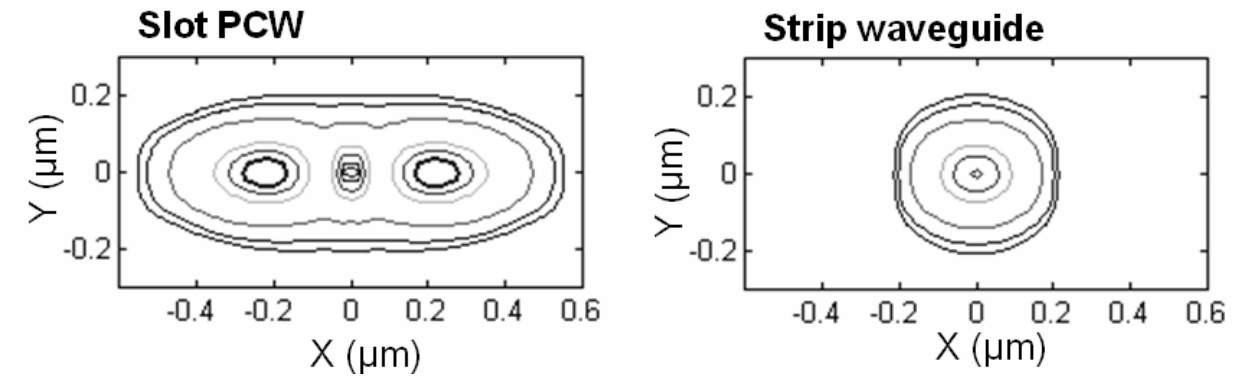

Fig. 3. Comparison of 2D field amplitude contours between a slot PCW and a single-mode strip waveguide.

The basic idea comes from the multimode power splitter structure that is often used to achieve equi-phase, balanced power partition from one single-moded input waveguide [17]. According to the principle of symmetric modal interference in a multimode waveguide [17]: the input signal excites the fundamental and second-order mode with different propagation constants; the total field profile is composed of the fundamental mode plus the second-order mode shifted by the phase difference. We can adjust the length of the multimode section to change the phase difference between 0 and π such that the resultant mode profile can best match the slot PCW. The schematic of the multimode interference coupler is shown in the inset of Fig. 4. The multimode section is designed to support two symmetric modes with W_M=1.6W. The single-moded input waveguide is centered with respect to the multimode section and will therefore excite only the even symmetric modes. With different L_M assumed, the coupling efficiency is estimated by the overlap integral between the output mode of the multimode section and the guided mode of the slot PCW. Calculation result is shown in Fig. 4 and shows that π phase difference of the even modes in the multimode waveguide provides the best coupling efficiency from the silicon strip waveguide to the slotted PCW. FDTD method is applied to simulate the evolution of transverse electric field and optical transmission along the propagation direction. The result is shown in Fig. 5. The multimode interference coupler is located between Z=0μm and Z=1.25μm. An efficient mode coupling from the conventional silicon strip waveguide to the novel slot PCW is confirmed.

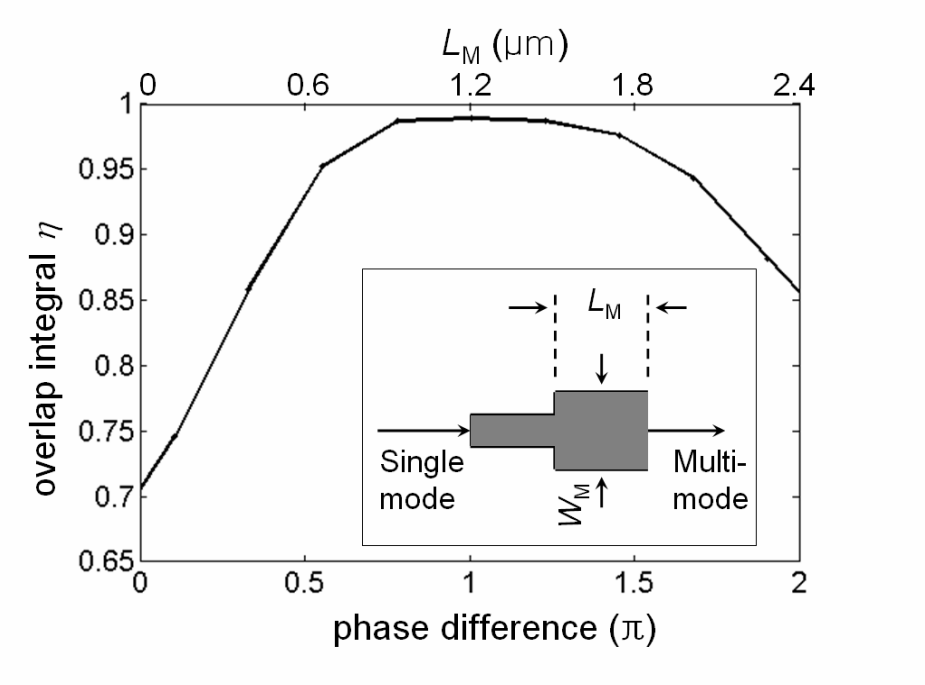

Fig. 4. Optimization of the mode overlap integral between the slot PCW and the multimode section. The integral is calculated as a function of the length of the multimode section and the phase difference of the excited even modes.

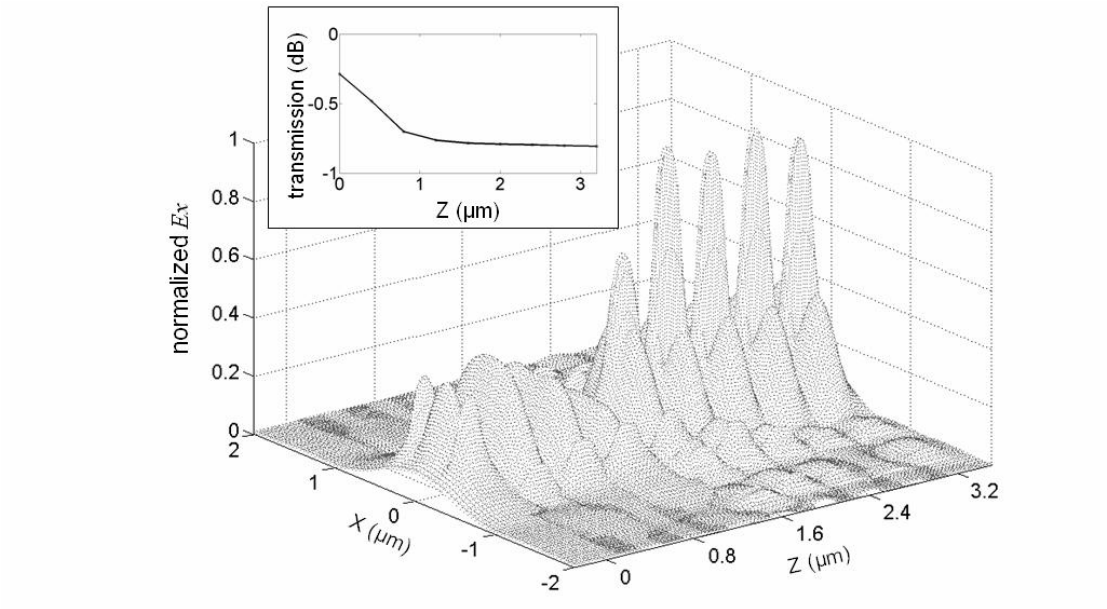

Fig. 5. A group of 3D Ex profiles in X-Y plane imaged at different Z positions. The transfer region begins at Z=0μm. The inset shows the transmission of the guided quasi-TE mode as a function of propagation distance.

IV. FABRICATION AND MEASUREMENT RESULT

The slot PCW with multimode interference coupler is fabricated on a silicon-on-insulator (SOI) wafer with a 1-μm buried oxide layer and a 250-nm top silicon layer. The slot nanostructure is formed in a hexagonal lattice photonic crystal slab with a=360/380nm and the hole diameter d=0.5a. Different lattice constants are employed to measure the optical transmission spectra for both guided mode and leaky modes of the waveguide. The waveguide slab layer is patterned using electron-beam lithography followed by reactive ion etching (RIE) and piranha cleaning. The crystal holes and the center void trench are then filled with spin-on-glass (SOG) material. The sample with coated SOG on top is postbaked at 425°C for 1 hour to achieve partial decarbonization. The refractive index of SOG after hard baking is n_{SOG}=1.42 that is close to low-index electro-optical materials. Figure 6 shows scanning electron microscopy (SEM) top-view pictures of the slotted photonic crystals before filling SOG. The SEM cross-section view of the waveguide structure shown in Fig. 7 confirms that all the void nanostructures in the waveguide slab layer have been filled with SOG. As the last step, an acrylic-based polymer layer that is transparent at 1.55 μm is coated to avoid symmetry-breaking background, where the guided modes can no longer be classified as even or odd and the band gap no longer exists [18].

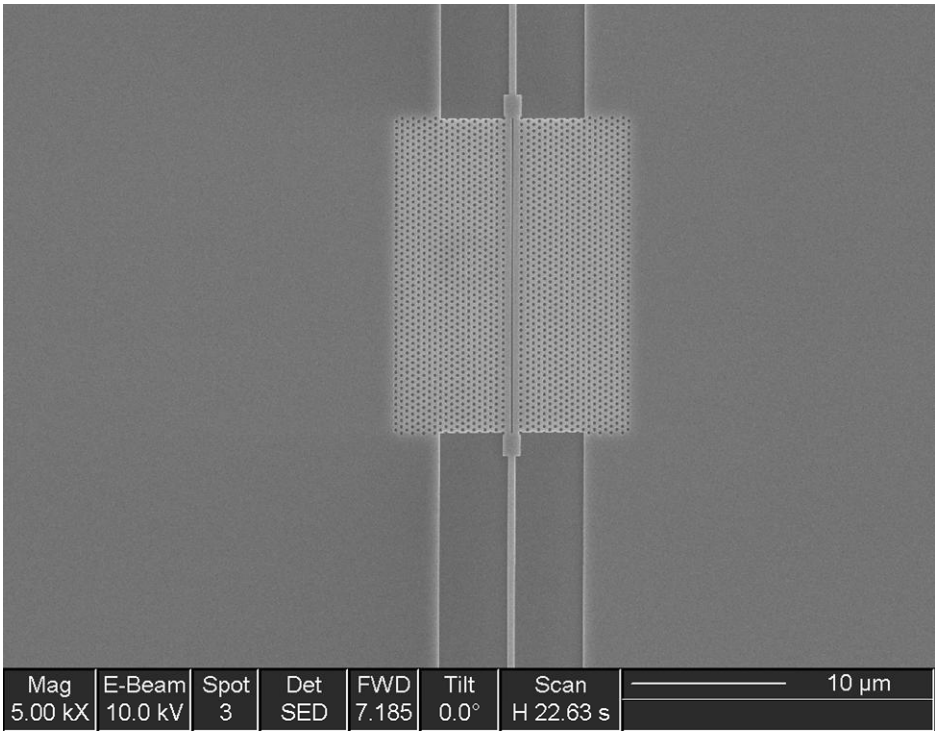

Fig. 6. Top-view SEM picture of a slot PCW integrated with two multimode interference couplers.

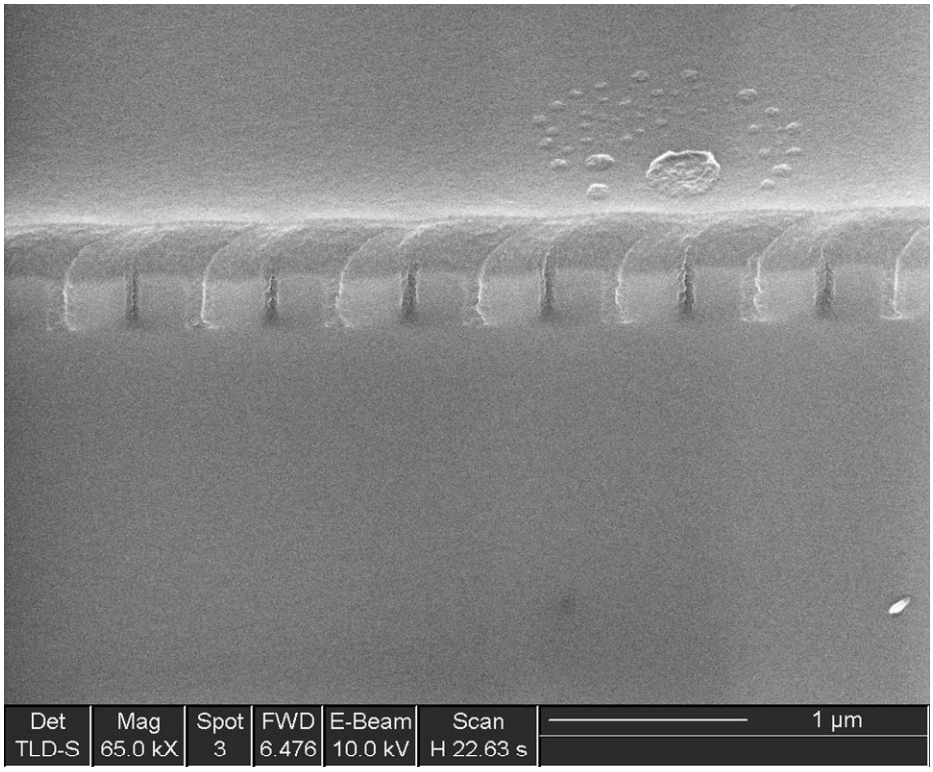

Fig. 7. Cross-section view of the slot PCW after filling SOG.

The experimental results of the optical spectra for both guided mode and leaky modes are shown in Fig. 8. Compared with direct coupling, one can find a 20dB efficiency enhancement for the guided mode when the coupling structure is employed. The insertion loss for the guided mode is less than 5dB. The measured band edge with slow light effect appears at the normalized frequency of 0.243. Comparing with the calculated band diagram for quasi-TE mode of the slotted photonic crystals, we can find good agreement between the simulated and experimental results. The frequency discrepancy is mainly due to the dimension difference between the simulated and fabricated waveguide structures. The mode mixing effect caused by the weak vertical asymmetry of the final device also induces some resonances in the spectrum [19].

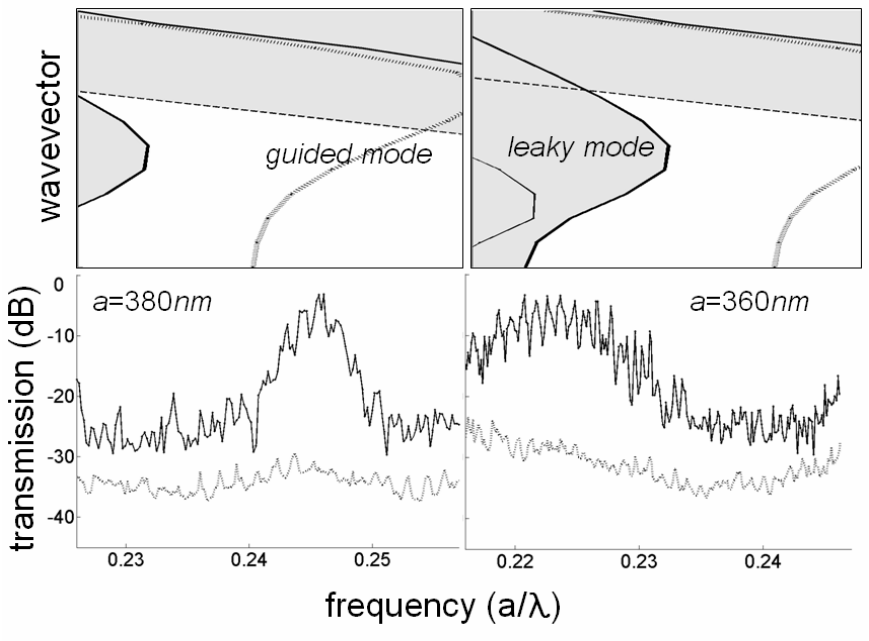

Fig. 8. Top panel: Enlarged portions of the photonic band structure for both guided and leaky modes. Bottom panel: transmission spectrum of the slot PCW of 320μm length with (solid) and without (dashed) coupling structures. The spectrum is normalized on transmission through a reference optical circuit.

V. CONCLUSION

In conclusion, we present a novel silicon-based slot photonic crystal structure and design a multimode interference-based compact mode converter with improved coupling efficiency. The slot photonic crystal waveguide exhibits low group velocity near the band edge and therefore leads to a significant enhancement of nonlinear effect for active devices. The waveguide structure demonstrated produces high electric field amplitude in a narrow low-index region and provides a feasible approach to apply low-index active materials in highly integrated optical circuits.

ACKNOWLEDGMENTS

This work is supported by AFOSR under Contract No. FA9550-05-C-0171 monitored by Dr. G. Pomrenke. Supports from DARPA, the State of Texas, and Sematech are also acknowledged. Nanofabrication and characterization facilities used for this work are partially supported by NSF and SPRING.

REFERENCES

1. Y. Jiang, W. Jiang, L. Gu, X. Chen, and R. T. Chen, Appl. Phys. Lett. 87, 221105 (2005).
2. Y. A. Vlasov, M. O'Boyle, H. F. Hamann, and S. J. McNab, Nature (London) 438, 65 (2005).
3. L. Gu, Y. Jiang, W. Jiang, X. Chen, and R. T. Chen, Proc. SPIE 6128, 261 (2006).
4. L. Gu, W. Jiang, X. Chen, L. Wang and R. T. Chen, Appl. Phys. Lett. 90, 071105 (2007).

5. M. Notomi, K. Yamada, A. Shinya, J. Takahashi, C. Takahashi, and I. Yokohama, Phys. Rev. Lett. 87, 253902 (2001).
6. M Soljacic, S. G. Johson S. Fan, M. Ibanescu, E. Ippen, and J. D. Joannopoulos, J. Opt. Soc. Am. B, 19, 2052 (2002).
7. M. Roussey, M. -P. Bernal, N. Courjal, D. V. Labeke, F. I. Baida and R. Salut, Appl. Phys. Lett. 89, 241110 (2006).
8. V. R. Almeida, Q. Xu, C. A. Barrios, and M. Lipson, Opt. Lett. 29, 1209 (2004).
9. Q. Xu, V. R. Almeida, R. R. Panepucci, and M. Lipson, Opt. Lett. 29, 1626 (2004).
10. W. T. Lau and S. Fan, Appl. Phys. Lett. 81, 3915 (2002).
11. S. Fan, P. R. Villeneuve, J. D. Joannopoulos, and E. F. Schubert, Phys. Rev. Lett. 78, 3294 (1997).
12. E. Chow, S. Y. Lin, S. G. Johnson, P. R. Villeneuve, J. D. Joannopoulos, J.-R. Wendt, G. A. Vawter, W. Zubrzycki, H. Hou, and A. Alleman, Nature (London) 407, 983 (2000).
13. S. G. Johnson, P. R. Villeneuve, S. Fan, and J. D. Joannopoulos, Phys. Rev. B 62, 8212 (2000).
14. Y. Wang, Z. Lin, J. Zhang, X. Cheng and F. Zhang, Appl. Phys. B 79, 879 (2004)
15. Z. Y. Li, L. L. Lin and K. M. Ho, Appl. Phys. Lett. 84, 4699 (2004).
16. M. Notomi, A. Shinya, K. Yamada, J. Takahashi, C. Takahashi, and I. Yokohama, IEEE J. Quantum Electron. 38, 736 (2002).
17. L. B. Soldano and E. C. Pennings, J. Lightwave Technol. 13, 615 (1995).
18. S. G. Johnson, S. Fan, P. R. Villeneuve, J. D. Joannopoulos, and L. A. Kolodziejski, Phys. Rev. B 60, 5751 (1999).
19. Y. A. Vlasov, N. Moll, and S. J. McNab, J. Appl. Phys. 95, 4538 (2004).